

**RECENT ACCELERATED WASTAGE OF THE MONTE PERDIDO GLACIER
IN THE SPANISH PYRENEES**

**López-Moreno, J.I.¹; Revuelto, J.¹, Rico, I.², Chueca-Cía, J.³, Julián, A.³, Serreta,
A.⁴, Serrano, E.⁵, Vicente-Serrano, S.M.¹, Azorín-Molina, C.¹, Alonso-González,
E.¹, García-Ruiz, J.M.¹**

1 Dept. Geoenvironmental Processes and Global Change, Pyrenean Institute of Ecology,
CSIC, Campus de Aula Dei, P.O. Box 13.034, 50.080-Zaragoza, Spain.

2 University of the Basque Country, Department of Geography, Prehistory and
Archeology, Vitoria, Spain

3 Dept. Geography. University of Zaragoza, Zaragoza, Spain.

4 Dept. Graphic Design and Engineering. University of Zaragoza, Huesca, Spain

5 Dep. Geography, University of Valladolid, Valladolid, Spain.

Corresponding author: nlopez@ipe.csic.es

Abstract

This paper analyzes the evolution of the Monte Perdido Glacier, the third largest glacier of the Pyrenees, from 1981 to the present. We assessed the evolution of the glacier's surface area by use of aerial photographs from 1981, 1999, and 2006, and changes in ice volume by geodetic methods with digital elevation models (DEMs) generated from topographic maps (1981 and 1999), airborne LIDAR (2010) and terrestrial laser scanning (TLS, 2011, 2012, 2013, and 2014). We interpreted the changes in the glacier based on climate data from nearby meteorological stations. The results indicate an accelerated degradation of this glacier after 1999, with a rate of ice surface loss that was almost three times greater from 2000 to 2006 than for earlier periods, and 1.85 times faster rate of glacier volume loss from 1999 to 2010 (the ice depth decreased by 8.98 ± 1.80 m, -0.72 ± 0.14 m w.e. yr⁻¹) compared to 1981 to 1999 (the ice depth decreased 8.35 ± 2.12 m, -0.39 ± 0.10 m w.e. yr⁻¹). This loss of glacial ice has continued at a lower rate from 2011 to 2014 (the glacier depth decreased by 1.93 ± 0.4 m, -0.58 ± 0.36 m w.e. yr⁻¹). These data indicated that two consecutive markedly anomalous wet winters and cool summers (2012-13 and 2013-14) resulted in a deceleration in wastage compared to previous 17 years, but were counteracted by the dramatic shrinkage that occurred during the dry and warm period of 2011-2012. Local climatic changes observed during the study period seems do not sufficiently explain the acceleration in wastage rate of this glacier, because precipitation and air temperature did not exhibit statistically significant trends during the studied period. The accelerated degradation of this glacier in recent years can be explained by the strong disequilibrium between the glacier and the current climate and probably other factors affecting the energy balance (i.e. increased albedo in spring) and feedback mechanisms (i.e. emitted heat from recent ice free bedrocks and debris covered areas).

Keywords: Glacier shrinkage, climate evolution, geodetic methods, terrestrial laser scanner (TLS), Pyrenees

1 Introduction

Most glaciers worldwide have undergone intense retreat since the culmination of the Little Ice Age (LIA) believed to have been in the mid 19th century, as indicated by measurements of ice surface area and volume (Vincent et al., 2013; Marshall 2014; Marzeion et al., 2014 and 2015; Zemp et al., 2014). This trend has apparently accelerated in the last three decades (Serrano et al., 2011; Mernild et al., 2013; Carturan et al. 2013a; Gardent et al., 2014; López-Moreno et al., 2014). Thus, Marshall (2014) and Zemp et al. (2015) noted that loss of global glacier mass during the early 21st century exceeded that of any other decade studied. Several studies examined this phenomenon in Europe. In the French Alps, glacier shrinkage has accelerated since the 1960s, mainly in the 2000s (Gardent et al., 2014). In the Ötztal Alps (Austria), Abermann et al. (2009) calculated the loss of glacier area was -0.4% per year from 1969 to 1997 and -0.9% per year from 1997 to 2006. In the Central Italian Alps, Scotti et al. (2014) compared the period of 1860-1990 with 1990-2007 and reported an approximately 10-fold greater average annual decrease of glacier area during the more recent period. Carturan et al. (2013b) also reported that the rate of ice mass loss in the long-term monitored Careser Glacier (Italian Alps) during the period 1981-2006 ($-1.3 \text{ m w.e. yr}^{-1}$) was about twice that for the period of 1933 to 1959 ($-0.7 \text{ m w.e. yr}^{-1}$). Over the same period (1980-2010), Fischer et al. (2015) calculated a very similar rate of ice mass loss for the Swiss Alps ($-0.65 \text{ m w.e. yr}^{-1}$) that clearly exceeds the values presented by Huss et al. (2010) for the 20th century (close to $-0.25 \text{ m w.e. yr}^{-1}$). In the

Sierra Nevada of southern Spain, the Veleta Glacier during the LIA, evolved into a rock glacier during the mid-20th century and has suffered marked degradation during the last two decades (Gómez-Ortiz et al., 2014).

The Pyrenees host some of the southernmost glaciers of Europe, and they have also undergone significant retreat (Grunewald and Scheithauer, 2010). In 2005, these glaciers had an area of 495 hectares (González-Trueba et al., 2008) and in 2008 they had a total area of 321 hectares (René, 2013). Since 1880, the different massifs have had variable reductions in area covered by ice, with a 59% reduction in the Vignemale Massif and an 84% reduction in the Posets-Llardana Massif (Gellatly et al., 1995; René, 2013). A total of 111 glaciers have disappeared in the Pyrenees from 1880 to 2005, and only 31 actual glaciers (with ice motion) remain. There has been a rapid glacial recession since the 1990s, and many of these glaciers face imminent extinction. Chueca et al. (2005 and 2008) reported that the rates of glacial shrinkage during the last two decades of the 20th century and the beginning of the 21st century were similar to those observed from 1860 to 1900, immediately after the end of the LIA. A similar conclusion has been reached by Marti et al. (2015) for the Ossoue Glacier (French Pyrenees).

Most studies agree that global warming is responsible for the observed glacier shrinkage and the recent acceleration of this shrinkage. The temperature increase has been particularly strong since the 1970s in most mountain ranges of the world (Haeberli and Beniston, 1998; Beniston et al., 2003; Nogués-Bravo et al., 2008; Gardent et al., 2014). Global warming has increased the equilibrium line altitudes (ELAs) and reduced the accumulation area ratios of glaciers, so that most glaciers are not in equilibrium with current climate (Mernild et al., 2013) and many of them cannot survive for much longer (Pelto, 2010). In the case of the Pyrenees, the annual air temperature has increased by a minimum of 0.9°C since the end of the LIA (Dessens and Bücher, 1998; Feullet and

Mercier, 2012). More recently, Deaux et al., (2014) reported an increase of 0.2°C decade⁻¹ for the period between 1951 and 2010. This explains the ~255 m increase in the elevation of the ELA of the glaciers of the Maladeta Massif since the end of the LIA, which is currently close to 2950 m a.s.l. (Chueca et al., 2005). The decreased accumulation of snow, and the increase on air temperature during the ablation season are thought to be the principal causes of recent glacier decline in the southern (Spanish) side of the Pyrenees (Chueca et al., 2005).

Glaciers are very good indicators of climate change due to their high sensitivity to anomalies in precipitation and air temperature (Carrivick and Brewer, 2004, Fischer et al., 2015). However, it is not always easy to establish a direct relation between annual fluctuations of climate and the changes in area and mass of a particular glacier. This is difficult because only glaciers of small size respond rapidly to changes in annual snowfall and snow/ice melt, whereas mid and large glaciers respond much more slowly (Marshall, 2014). Moreover, very small glaciers may develop and evolve for reasons unrelated to the regional long-term, monthly or seasonal climatic evolution, such as avalanches, wind drifting and new rock exposures. In the case of shrinking glaciers the latter can be key (Chueca et al. 2004; Serrano et al., 2011; Carturan et al., 2013c). Local topography also has a considerable effect on the development of ice bodies, and can cause notable variations in the ELAs of different glaciers in the same region (Reinwarth and Escher-Vetter, 1999; Carrivick and Brewer, 2004; López-Moreno et al., 2006). Moreover, many studies of recent changes in glaciers examined the evolution of the area of glaciated surfaces or glacier lengths. These parameters respond to climate fluctuations, although this relationship is also affected by geometric adjustments (Haeberli, 1995; Carturan et al., 2013a). Thus, direct mass-balance estimations or geodetic methods that determine changes in ice volume provide better information on

the relationship between glacier changes and climatic changes (Chueca et al., 2007; Cogley, 2009; Fischer et al., 2015). In the Pyrenees, there are very few estimations of ice volume loss (Del Río et al., 2014; Sanjosé et al., 2014; Marti et al., 2015), although abundant research has examined recent changes of glaciated surface areas (Chueca et al., 2005, López-Moreno et al. 2006; González-Trueba et al., 2008). Annual estimates of glacier mass fluctuations based on the glaciological method were only performed on the Maladeta Glacier (Spanish Pyrenees) and on the Ossoue Glacier (French Pyrenees), and these indicated the mean glacier thinning was -14 m during the last 20 years on the Maladeta Glacier, and -22 m on the Ossoue Glacier (Arenillas et al., 2008; René, 2013; Marti et al., 2015). Other studies in the Spanish Pyrenees compared digital elevation models (DEMs) derived from topographic maps of 1981 and 1999 in the Maladeta Massif (Chueca et al., 2008) and the Monte Perdido Glacier (Julián and Chueca, 2007), and reported losses of -0.36 m w.e. yr⁻¹ and of -0.39 m w.e. yr⁻¹, respectively.

This paper focuses on the recent evolution of the Monte Perdido Glacier, the third largest glacier in the Pyrenees. We document changes in the glacier surface area from 1981 to 2006 and provide updated information on volumetric changes by comparing DEMs derived from topographic maps of 1981 and 1999 (Julian and Chueca, 2007), a new DEM obtained in 2010 from Airborne LIDAR, and four successive Terrestrial Laser Scanning (TLS) surveys that were performed during the autumns of 2011, 2012, 2013, and 2014. We examined these data in connection with data on precipitation, snow depth, and air temperature from the closest meteorological station. Identification of changes during recent years in this region is particularly important because in the 21st century snowfall accumulation has been higher and the temperatures slightly cooler than in the last decades of the 20th, associated to a persistently positive North Atlantic Oscillation index in the beginning of the 21st century (Vicente-Serrano et al., 2010;

Buisan et al., 2015). Thus, the most recent response of the remnant ice bodies to this climatic anomaly is as yet unknown. Moreover, the availability of annual TLS data in recent years permits detailed examination of the relationship between changes in climate and glaciers.

2 Study area and review of the previous research on the Monte Perdido glacier

The Monte Perdido Glacier (42°40'50"N 0°02'15"E) is located in the Ordesa and Monte Perdido National Park (OMPNP) in the Central Spanish Pyrenees (Figure 1). The ice masses are north-facing, lie on structural flats beneath the main summit of the Monte Perdido Peak (3355 m), and are surrounded by vertical cliffs of 500-800 m in height (García-Ruiz and Martí-Bono, 2002). At the base of the cliffs, the Cinca River flows directly from the glacier and the surrounding slopes, and has created a longitudinal west-east basin called the Marboré Cirque (5.8 km²).

Researchers have studied glaciers in the Marboré Cirque since the mid 19th century (Schrader, 1874), and many subsequent studies examined the extent and made descriptions of the status of the ice masses and the features of the moraines deposited during the LIA (Gómez de Llarena, 1936; Hernández-Pacheco and Vidal Box, 1946; Boyé, 1952). More recent studies have established the location of moraines to deduce the dynamics and extent of LIA glaciers (Nicolás, 1981 and 1986; Martínez de Pisón and Arenillas, 1988; García Ruiz and Martí Bono, 2002; Martín Moreno, 2004) and have analyzed environmental changes during the Holocene through the study of sediments in Marboré Lake (Oliva-Urcia et al., 2013) and by dating of Holocene morainic deposits (García-Ruiz et al., 2014).

1 The map of Schrader (1874), numerous old photographs, and the location of the LIA
2 moraines (García Ruiz and Martí Bono, 2002) indicate a unique glacier at the foot of the
3 large north-facing wall of the Monte Perdido Massif (Monte Perdido, Cilindro and
4 Marboré peaks) (Figure 1). The map of Schrader (1874) distinguishes the Cilindro-
5 Marboré Glacier, with three small ice tongues that joined in the headwall, from the
6 Monte Perdido Glacier, which was divided into three stepped ice masses connected by
7 serac falls until the mid 20th century. The glacier that existed at the lowest elevation
8 was fed by snow and ice avalanches from the intermediate glacier, but disappeared after
9 the 1970s (Nicolas, 1986; García-Ruiz et al., 2014). The two remaining glacier bodies,
10 which are currently unconnected, are referred to this paper as the upper and lower
11 Monte Perdido Glaciers. The glacier beneath the Cilindro and Marboré peaks has
12 transformed into three small and isolated ice patches (García-Ruiz et al., 2014). It is
13 noteworthy that Hernández-Pacheco and Vidal Box (1946) previously estimated a
14 maximum ice thickness of 52 m for the upper glacier and 73 m for the lower glacier. In
15 2008, 82% of the ice cover at the end of the LIA had already disappeared. The upper
16 and lower ice bodies have mean elevations of 3110 m and 2885 m (Julián and Chueca,
17 2007). Despite the high elevation of the upper glacier, snow accumulation is limited due
18 to the minimal avalanche activity above the glacier and its marked steepness ($\approx 40^\circ$).

19 There has not been a direct observation of the current location of the ELA in the upper
20 Cinca valley, but studies at the end of the 20th and beginning of the 21st century placed
21 it at about 2800 m in the Gállego Valley, west of the OMPNP (López-Moreno, 2000),
22 and at about 2950 m in the Maladeta Massif, east of the OMPNP (Chueca et al., 2005).
23 The mean annual air temperature at the closest meteorological station (Góriz at 2250 m
24 a.s.l., 2.7 km from the glacier) is 5.03°C, although this station is on the south-facing
25 slope of the Monte Perdido Massif. Assuming a lapse rate of 0.55°C to 0.65°C every

1 100 m, the annual 0°C isotherm should be roughly at 2950 to 3150 m a.s.l. The climate
2 in this region can be defined as high-mountain Mediterranean. Precipitation as snow can
3 fall on the glacier any time of year, but most snow accumulation is from November to
4 May, and most ablation is from June to September.

6 **3 Data and methods**

7 **3.1. Comparison of DEMs**

8 DEMs from different dates can be used to calculate changes in glacier ice volume. This
9 technique is well established for the study of glaciers in mountainous areas (Favey et
10 al., 2002), and we have previously applied it in several studies of the Pyrenees (Chueca
11 et al., 2004, 2007; Julián and Chueca, 2007). Thus, we used three DEMs to estimate the
12 changes in ice volume in the Monte Perdido Glacier. Two DEMs (1981 and 1999) were
13 derived from topographic maps and one (2010) was from airborne LIDAR
14 measurements. All three DEMs have a cell size of 2x2 m, and they were used in the
15 context of a geographic information system (GIS), working under the European Datum
16 ED50 (UTM projection, zone 30).

17 The 1981 DEM was obtained from the cartography published by the Spanish *Instituto*
18 *Geográfico Nacional* (IGN) (Sheet 146-IV, Monte Perdido; Topographic National Map
19 Series, scale 1:25000). This map was published in 1997 and its cartographic restitution
20 was based on a photogrammetric flight in September 1981. The 1999 DEM was also
21 derived from cartography published by the IGN (Sheet 146-IV, Monte Perdido;
22 Topographic National Map Series MTN25, scale 1:25000). It was published in 2006
23 and its cartographic restitution was based on a photogrammetric flight in September
24 1999. The 2010 DEM was obtained from an airborne LIDAR flight (MDT05-LIDAR)

made by the IGN in September of 2010 in the context of the National Plan for Aerial Orthophotography (NPAO).

The Root Mean Squared Error (RMSE) for elevation accuracy calculated by the IGN for their digital cartographic products at 1:25000 scale is ± 1.5 m and ± 0.2 m for their LIDAR derived DEMs. To verify these accuracies we made a comparison of 2010-1999, 2010-1981 and 1999-1981 pairs of DEMs in areas of ice-free terrain placed near the studied glaciers. The results showed good agreement with the accuracy indicated by the IGN in almost all areas although larger vertical errors were identified in several sectors of very steep terrain (with slope values usually $> 65^\circ$) located in the Monte Perdido glacial cirque (sharp-edged crests and abrupt cliffs linked to the geological and structural disposition of the area). In those sectors, differences between the DEMs reached 10-15 m. As both Upper and Lower Monte Perdido glaciers are placed well outside those areas and have smoother topographical surfaces it might be assumed that the altimetric data provided by the IGN has an appropriate consistency over glaciated terrain.

The combined vertical RMSE for DEM differences was < 2.5 m for 1999 minus 1981 and < 2.0 m for 2010 minus 1999. In the latter case it must be noted that different geodetic methods (photogrammetrical and airborne LIDAR) were used in the comparison and that this fact could alter the accuracy of the elevation changes (Rolstad and others, 2009). In any case, both these errors were considered precise enough for our purposes as the ice-depth changes obtained in our analysis were generally much higher than these values. The estimation of ice volume changes was performed in ArcGIS comparing, by cut and fill procedures, pairs of glacier surface DEMs (1981-1999 and 1999-2010). The glacial perimeters associated with each DEM date were retrieved from aerial photographs (1981: *Pirineos Sur* Flight, September 1981, scale of 1:30000, black

and white; 1999: *Gobierno de Aragón* Flight, September 1999, scale of 1:20000, color).

There were no high quality flights for 2010, so 2006 aerial photographs were used (PNOA2006 Flight, August 2006, scale of 1:5000, color). The 1999 and 2006 photographs were already orthorectified, but we had to correct the geometry and georeference the aerial survey of 1981 by use of the georeferencing module of ArcGIS. The reference for the control points was from the orthophotos and DEM data from 1999. The horizontal RMSE accuracy of the set of control points ranged from 2.1 to 4.7 m, and was considered sufficiently precise for our study. The maximum horizontal error was used to calculate the uncertainty of glacierized areas and their temporal changes. This uncertainty was calculated using the *buffer* tool in ArcGIS. This tool allowed quantifying the area of the polygon generated with the maximum horizontal error around the perimeter of the glacier. A resampling procedure using cubic convolution was used to generate the final rectified images.

The most recent estimates of the evolution of the glacier were from annual TLS surveys. LIDAR technology has developed rapidly in recent years, and terrestrial and airborne LIDAR have been used in diverse geomorphology studies, including monitoring changes in the volume of glaciers (Schwalbe et al. 2008, Carturan et al., 2013b). The device used in the present study is a long-range TLS (RIEGL LPM-321) that uses time-of-flight technology to measure the time between the emission and detection of a light pulse to produce a three-dimensional point cloud from real topography. The TLS used in this study employed light pulses at 905 nm (near-infrared), which is ideal for acquiring data from snow and ice cover (Prokop, 2008, Grünwald et al., 2010; Egli et al., 2011), a minimum angular step of 0.0188°, a laser beam divergence of 0.0468°, and a maximum working distance of 6000 m.

When TLS is used for long distances, various sources of error must be considered, namely the instability of the device and errors from georeferencing the point of clouds (Reshetyuk, 2006). We used an almost frontal view of the glacier (same as for the photos shown in Figure 4) with minimal shadow zones in the glacier and a scanning distance of 1500 to 2500 m. We also used indirect registration, also called target-based registration (Revuelto et al., 2014), so that scans from different dates (September of 2011 to 2014) could be compared. Indirect registration uses fixed reference points (targets) that are located in the study area. 11 reflective targets of known shape and dimension (cylinders of 10x10 cm for those located closer than 200 meters, and squares of 50x50 cm for longer distances) were placed at the reference points on rocks at a distance from the scan station of 10 to 500 m. Using standard topographic methods, we obtained accurate global coordinates for the targets by use of a differential global positioning system (DGPS) with post-processing. The global coordinates were acquired in the UTM 30 coordinate system in the ETRS89 datum. The final precision for the set of target coordinates was ± 0.05 m in planimetry and 0.10 m in altimetry. A total of 65 reference points around the ice bodies (identifiable sections of rocks and cliffs) were used to assess measurement accuracy. Ninety percent of the reference points had an error lower than 0.40 m. Such 40 cm of error was considered as the uncertainty (error bars) to the calculated ice depth and mass loss rates. The conversion of mean ice elevation change to annual mass budget rates was done applying mean density of 900 kg m^{-3} (Chueca et al., 2007; Marti et al., 2015). The assumption of this value neglects the existence of firn, with a lower density. This is mostly true at the end of the study period, but probably in the early eighties this assumption is not completely true and firn areas existed (i.e. according to Figure 3A). Unfortunately, the lack of additional

information forced us to adopt this generalization that may slightly overestimate the mass loss rate for 1981–1999.

3.2 Climatic data

The Spanish Meteorological Office (AEMET) provided climatic data from the Góriz manual weather station, located at 2250 m a.s.l. on the southern slope of the Monte Perdido Massif. The absence of changes in instrumentation and observation practices in the meteorological station since 1983, and the proximity of the meteorological station to the glacier (2.7 km), suggests that it accurately records the climate variability over the glacier. The climatic record consists of daily data of air temperature, precipitation, and snow depth. From these data, we derived annual series of maximum and minimum air temperatures for the main periods of snow accumulation (November-May) and ablation (June-September), precipitation during the accumulation season, and maximum snow depth in April (generally the time of maximum snowpack at this meteorological station). The lack of detailed meteorological or mass balance data over the glacier made it necessary to define the accumulation and the ablation seasons in a subjective manner based on our experience. We are aware that May and October are transitional months between accumulation and ablation conditions depending on specific annual conditions.. However, we set these periods because June and November are the months when ablation and accumulation respectively become generally evident over the surface of the glacier. The statistical significance of the linear climate trends was assessed by the non-parametric correlation coefficient of Mann-Kendalls tau-b (Kendall and Gibbons, 1990). Results obtained for Góriz were contrasted with those from three other observatories (see Figure 1) with precipitation (Pineta, Aragnouet and Canfranc), and temperature

(Mediano, Aragnouet and Canfranc) data for the period 1983 and 2013, and also for 1955-2013. The non-parametric Mann-Whitney U test (Fay and Proschan, 2010) was used to detect statistically significant differences in the medians of precipitation and temperature when the periods 1983-1999 and 2000-2010 are compared.

4. Results

4.1. Climatic evolution and variability from 1983 to 2014

Figure 2 illustrates the high interannual variability of climate at Góriz station since 1983. The average maximum air temperatures at Góriz during the snow accumulation and ablation seasons had no significant trends, with tau-b values close to 0 (Figs 2a and 2b). The range between the highest and lowest average seasonal anomalies during the study period exceeded 3°C and 4°C during the accumulation and ablation periods, respectively for maximum and minimum temperatures. The average minimum air temperatures had very weak increases in both seasons, but these were not statistically significant ($p < 0.05$). The interannual air temperature range was larger for the accumulation period (~5°C) than for the ablation period (~2.5°C). Table 1 shows that the evolution of temperature at Góriz is line with that observed at the three other meteorological stations (Mediano, Aragnouet and Canfranc). They do not exhibit statistically significant trends for maximum or minimum temperature during the period 1983-2013. On a monthly basis, the four analysed observatories only exhibited a statistically significant increases in May and June; and statistically significant decreases of maximum and minimum temperature in November and December. The Mann-Whitney test did not reveal statistically significant differences in the medians of the

series for the accumulation and ablation seasons at any observatory when the periods 1983-1999 and 2000-2010 were compared.

Precipitation at Góriz during the accumulation period also exhibited strong interannual variability, with a range of ~ 600 mm to 1500 mm (Fig. 2e). The trend line had a slight increase, but this was not statistically significant. Similarly, maximum snow accumulation during April varied from less than 50 cm to 250 cm, and there was no evident trend during the study period (Fig. 2f). Monthly trend analysis (Table 1) only found a significant increase of precipitation at Góriz during May, and near zero tau-b coefficients for the most of the months. Very similar results are found for the other three analyzed stations (Pineta, Aragnouet and Canfranc) with no statistically significant trends for the accumulation and ablation periods. Only Aragnouet showed a statistically significant increase in May, and Pineta in March. No statistically significant differences in the median of precipitation during the accumulation and ablation seasons of the 1983-1999 and 2000-2010 periods were found at any of the analyzed meteorological stations.

In addition, Figure 3 shows the interannual evolution of temperature and precipitation series for a longer time slice (1955-2013). They illustrate that climate observed during the main studied period (1983-2013) is not necessarily representative of the longer climate series. Thus, the 1955-2013 period exhibits a statistically significant ($p<0.05$) warming during the ablation period, and the accumulation exhibited positive tau-b values but did not reach statistical significance. Precipitation during the accumulation period did not exhibit statistically significant trends during the period 1955-2013 in any of the three analyzed observatories.

Figure 2 also shows that the last three years, for which we have TLS measurements of annual glacier evolution, had extremely variable conditions. Thus, mid-September 2011

to mid-September 2012 was one of the warmest recorded years (especially during the ablation period, 96th and 74th percentiles for maximum and minimum temperature) and with a rather dry accumulation period (27th percentile). The period of 2012 to 2013 had an accumulation period that was more humid than average (59th percentile) and the coolest recorded summer (1st and 18th percentiles for maximum and minimum temperatures respectively), and the accumulation period of 2013 to 2014 was very wet (78th percentile) and slightly cooler than average respectively, with air temperatures around or below the average (22th and 48th percentiles for maximum and minimum temperature respectively) during the ablation months.

4.2 Glacier evolution from 1981 to 2010

Figure 4 shows two photographs of the glacier taken in late summer of 1981 and 2011. A simple visual assessment shows the fast degradation of the glacier during this 30 year period. In 1981, the upper and lower glaciers were no longer united (they became disconnected between 1973 and 1978), and they exhibited a convex surface and a significant ice depth with noticeable seracs hanging from the edge of the cliffs. Both ice bodies were heavily crevassed, with evidence of ice motion over the whole glacier. The photograph of 2011 shows that the two ice bodies are further separated, as well as showing a dramatic reduction in ice thickness, manifested by the concave surface, the disappearance of almost all seracs, and the retreat of ice from the edges of the cliffs. Crevasses are only evident in the eastern part of the lower glacier, indicating that the motion of the glacier has slowed or stopped in most of these two ice bodies. Moreover, there are rocky outcrops in the middle of the lower glacier and areas that are partially covered by debris deposits from several crevasses or rock falls in the upper areas.

Table 2 shows the surface area of the ice in 1981, 1999, and 2006. From 1981 to 1999 the glacier lost 4.5 ± 0.19 ha (-1.5 ± 0.06 ha in the upper glacier and -3.0 ± 0.13 in the lower glacier), corresponding to an overall rate of -0.25 ± 0.01 ha yr⁻¹. From 1999 to 2006, the glacier losses were 5.4 ± 0.24 ha (-2.0 ± 0.09 ha in the upper glacier and -3.4 ± 0.15 ha in the lower glacier), corresponding to an overall rate of -0.77 ± 0.23 ha yr⁻¹, more than three times the rate of the previous 18 years.

Comparison of the elevation of the glacier's surfaces derived from the DEMs (1981 to 1999 vs. 1999 to 2010) also indicates an acceleration of glacier wastage over time (Figure 5). During the 1981-1999 period, the ice thickness decreased by an average of 6.20 ± 2.12 m in the upper glacier and 8.79 ± 2.12 m in the lower glacier (-8.35 ± 2.12 m overall); thus, the mean rate of glacier thinning was 0.34 ± 0.11 m and 0.48 ± 0.11 m yr⁻¹ (-0.46 ± 0.11 m yr⁻¹ overall, or -0.39 ± 0.1 m w.e. yr⁻¹) respectively. Moreover, the changes in glacier thickness had spatial heterogeneity. No sectors of either glacier had increased thicknesses, but some small areas of the lower glacier remained rather stationary, with declines in thickness less than 5 m. The largest losses of glacier thickness were in the lower elevations and western regions of the upper and lower glaciers, with decreases that exceeded 25 m and 35 m respectively. During the 1999-2010 period, the thinning was 7.95 ± 1.8 m in the upper glacier and 9.13 ± 1.8 m in the lower glacier (-8.98 ± 1.8 m overall); corresponding to rates of -0.72 ± 0.16 m and -0.81 ± 0.16 m yr⁻¹ (-0.8 ± 0.16 m yr⁻¹ overall, or -0.72 ± 0.14 m w.e. yr⁻¹) respectively. The spatial pattern of thinning resembled the pattern from 1981-1999, but areas of noticeable glacier losses are also found eastward. The smallest decreases are found in the higher elevation parts of the lower glacier and the proximal area of the upper glacier, probably due to most effective shading of these areas, and the greatest decreases in the distal and central-eastern parts of both ice bodies.

4.3. Evolution of Monte Perdido Glacier from 2011 to 2014 from TLS measurements

Figure 6 shows the differences in glacier depth between consecutive annual scans (September 2011-12, September 2012-13, and September 2013-14) and the total change from 2011 to 2014. Figure 7 shows the frequency distribution of ice depth change measured over the glacier for these periods.

The period of mid-September 2011 to mid-September 2012 was very dry during the accumulation period and very warm during the ablation period. These conditions led to dramatic glacier thinning, with an average decrease of 2.1 ± 0.4 m (-2.08 ± 0.4 m in the upper glacier and -2.12 ± 0.4 m in the lower glacier). Ice thinning affected almost the entire glacier (the accumulation area ratio, AAR, was 3.5%), and was particularly intense in the western sectors of the upper and lower glaciers, where losses were more than 4 ± 0.4 m. The few scattered points indicating depth increases in the middle of the lower glacier are likely to be from the motion of the existing crevasses.

Conditions were very different from 2012 to 2013, with a rather wet accumulation period and very cool ablation period. These conditions led to changes that contrasted sharply with those of the previous year, in that large areas of the glacier had increased ice thickness. Most of these increases did not exceed 1.5 ± 0.4 m, and most were in the highest elevation areas of both ice bodies. Nonetheless, during this year, large areas remained stable (AAR was 54%) and some areas even exhibited noticeable ice losses (more than $1.5-2 \pm 0.4$ m in the upper and lower glaciers). Despite the excellent conditions for glacier development from 2012 to 2013, the average increase of glacier thickness was only 0.34 ± 0.4 m ($+0.32 \pm 0.4$ m in the upper glacier and $+0.38 \pm 0.4$ m in the lower glaciers). Very similar conditions occurred in 2013-2014, with very wet

accumulation months and below average air temperature during the ablation period. Again, there were large areas with moderate increases in thickness (AAR was 41%, sometimes exceeding 3 m), although there were still areas with significant ice loss, with an average depth decrease of 0.07 ± 0.4 m (-0.08 ± 0.4 m in the upper glacier and -0.07 ± 0.4 m in the lower glacier).

The overall result of a very negative year (2011-2012) for glacier development followed by two years (2012-2013 and 2013-2014) of anomalous positive conditions led to a net average ice loss of 1.93 ± 0.4 m (-0.58 ± 0.36 m w.e. yr^{-1}), with some regions experiencing losses greater than 6 ± 0.4 m. Only the areas of the eastern part of the lower glacier that were at high elevations (around the bergschrund) exhibited some elevation gain during this period (accumulation area ratio, AAR, for the three years was 16%), and this was typically less than $+2 \pm 0.4$ m. Interestingly, the areas with greatest and lowest ice losses during 1981-2010 were similar to those with the greatest and lowest ice losses during 2011-2014, indicating a consistent spatial pattern of glacier shrinkage over time.

5. Discussion and conclusions

The results of this study indicate that the recent evolution of the Monte Perdido Glacier was similar to that of many other glaciers worldwide (Marshall, 2014; Vincent et al., 2013), especially those in Europe (Gardent et al., 2014; Abermann et al., 2009; Scotti et al., 2014; Marti et al., 2015) where glacier shrinkage after the culmination of the LIA and has clearly accelerated after 2000. More specifically, the annual loss of area of the Monte Perdido Glacier was three-times greater from 2000 to 2006 compared to the 1981-1999 period; and the glacier thinning from 1999 to 2010 was double that observed from 1981 to 1999. Acceleration in glacier shrinkage has been also reported

for the Ossoue Glacier (French Pyrenees), where mass balance during the period 2001-2013 ($-1.45 \text{ m w.e. yr}^{-1}$) is 50% greater compared to the period 1983-2014 ($-1 \text{ m w.e. yr}^{-1}$), (Marti et al., 2015). Climatic analyses suggest that the recent acceleration in the wastage of the Monte Perdido Glacier cannot be only explained by an intensification of climate warming or by a decline of snow accumulation. Climate data (1983-2014) of a nearby meteorological station, and three other Pyrenean meteorological stations, suggests that during most of the year temperature has not exhibited statistically significant trends. The Mann-Whitney test did not reveal statistical differences in temperature when the period 1983-1999 was compared to 1999-2010. Precipitation in the four analyzed stations during the accumulation period and maximum annual snow depth at Góriz were also stationary or slightly increased. Previous studies of the Pyrenees and surrounding areas showed that air temperature has significantly warmed throughout the 20th century, especially after the relatively cold period from the 1960s to the mid-1970s (López-Moreno et al., 2008; El Kenawy et al., 2012; Deaux et al., 2014). Such changes have been also detected in the three temperature series analyzed for this study during the period 1955-2013. At the same time, there was a regional significant decline of snow accumulation from mid-March to late-April/early-May from 1950 to 2000 in the Pyrenees (López-Moreno, 2005). These trends of decreasing precipitation and milder air temperatures during winter and early spring were related to changes in the North Atlantic Oscillation (NAO) index during this period (López-Moreno et al., 2008). Most recent studies that used updated databases (including data of the 21st century) confirmed that a shift towards more negative NAO has affected the recent evolution of temperature and precipitation over the Pyrenees. Thus, no temporal trends of either variable are found near Monte Perdido since the 1980s, when the study period starts in the 1980s and the effect of the cold and wet period of the 1960s to 1970s is

1 removed. Vicente-Serrano et al. (2010) found that the increased occurrence of very wet
2 winters during the 2000s was associated with frequent strong negative NAO winters. In
3 agreement, Buisan et al. (2015) indicated that for the period of 1980 to 2013 the overall
4 number of snow days in the Pyrenees remained stationary and even slightly increased in
5 some locations. In a most recent study, Buisan et al. (under review) has reported
6 stationary behavior or slight increases in snow water equivalent for the period 1985-
7 2015 in the central Spanish Pyrenees. Macias et al. (2014) support the view that
8 southern Europe and some other regions of the world have undergone clear moderations
9 of the warming trends that were reported at the end of the 20th century. Nonetheless, it is
10 necessary to bear in mind that the longest climatic records or dendroclimatological
11 reconstructions for the Pyrenees still point out the period considered in this study (1980-
12 2014) as a very strong positive anomaly of temperature and a dry period compared to
13 the period since the end of the LIA (Büntgen et al., 2008; Deaux et al., 2014; Marti et
14 al., 2015). More research is needed to fully assess the implications of the temperature
15 increase detected in May and June in the four analyzed meteorological stations. This
16 change could lead to less snow accumulation at the end of the accumulation season and
17 a longer ablation period, and an early rise of albedo that may be affecting the mass and
18 energy balance of the glacier (Qu et al., 2014). Another hypothesis that should be
19 considered in future research is to consider the effect of increasing slope of the glaciers,
20 due to higher thickness loss in the distal parts. Increasing slopes are expected to affect
21 snow accumulation on the glaciers and might constitute another feedback mechanism to
22 explain the recent evolution of the glacier.

23 The mass loss rates presented in this study for the different periods (-0.39 ± 0.1 and -
24 0.72 ± 0.14 m w.e. yr^{-1} for 1980-1999 and 1999-2010 periods respectively) are similar to
25 the reported by Chueca et al., (2007) and Marti et al. (2015) for the Maladeta massif (-

0.36 m w.e. yr⁻¹ for the 1981-1999 period; and -0.7 m w.e. yr⁻¹ for the 1991-2013). The most recent mass balance values obtained for the Monte Perdido Glacier are more similar to those reported for the Swiss Alps (Fischer et al., 2015), or the best preserved glaciers in some areas of the Italian Alps (Carturan et al., 2013 a); but lower than those of the fastest retreating glaciers in the Alps (Carturan et al., 2013b) or that reported for the Ossoue Glacier (French Pyrenees, -1.45 m w.e. yr⁻¹ for the 1983-2014). The smaller rates on the Spanish side of the Pyrenees than on the French side may be explained by the location of the remnant ice bodies on Southern side of the range, confined to the most elevated and the least exposed locations in their respective cirques (López-Moreno et al., 2006). In contrast, the Ossue glacier has maintained a considerable glacier tongue on an eastward slope. In this context, the only explanation for the rapid degradation of the Monte Perdido Glacier after 1999 is that the progressive warming observed since the end of the LIA was responsible for a dramatic reduction in the accumulation area ratio (AAR), and most of this glacier is below the current ELA (at 3050 m a.s.l. during the three-year period 2011-2014, Figure 6D). This leads to a clear imbalance that is very likely to be exacerbated by negative feedbacks. Because of this imbalance, the glacier cannot recover ice losses during periods with favorable conditions (high accumulation and/or little ablation in the frame of the 1983-2014 period). This hypothesis is strongly supported by our detailed TLS measurements from the last four years. In particular, these TLS data showed that two consecutive anomalously positive years (2012/13 and 2013/14), compared to a period with unfavourable conditions for the glaciers, did not allow recovery of the losses from a negative year (2011/12). Thus the glacier thinning during this three years period was 1.93 ± 0.4 m (-0.58 ± 0.36 m w.e. yr⁻¹), roughly one-fourth of the loss from 1981 to 1999, and from 1999 to 2010. The accumulation area ratio for the 2011-2014 period was 16 %, and during a warm and dry year the loss of ice

1 thickness affects almost the whole glacier ($AAR < 4\%$) indicating that there is not a
2 persistent accumulation zone. Pelto (2010) observed that this is a symptom of a glacier
3 that cannot survive. There can be years with mass gain, but there is loss in most years
4 and the retained snowpack of good years is lost in bad years, then in fact there is no
5 cumulative accumulation. Thus, the behavior observed for the Monte Perdido glacier
6 during the studied period is very likely explained by very negative mass balance years
7 that may be identified in Figure 2. Thus, years with very high temperatures occurred
8 after 2000 (2003, 2005 and 2012), and in 2005 and 2012 they were also characterized
9 by low winter precipitation. The feedbacks from decreased albedo and increasing slope
10 of the glaciers may also be playing a key role in the recent acceleration of the glacier
11 wastage. Obviously, this indicates that the future of the Monte Perdido Glacier is
12 seriously threatened, even under stationary climatic conditions. A ground-penetrating
13 radar (GPR) survey of the lower glacier in 2010 reported a maximum ice depth close to
14 30 m in the westernmost part of the lower glacier (unpublished report), suggesting that
15 large areas of this glacier may even disappear within the next few years. This process
16 may be accelerated by negative feedbacks such as the recent rise of rocky outcrops in
17 the middle of the glacier and the thin cover of debris, both of which may accelerate
18 glacier ablation by decreasing the albedo and increasing the emissivity of long-wave
19 radiation. The highly consistent spatial pattern of ice losses in the last 30 years suggests
20 that the westernmost part of this glacier will disappear first; the easternmost part will
21 survive longer as a small residual ice mass because of greater snow accumulation during
22 positive years and a lower rate of degradation. When the glacier is restricted to this
23 smaller area, it is likely that its rate of shrinkage will decrease, as observed for other
24 Pyrenean glaciers (López-Moreno et al., 2006).

1 The future long-term monitoring of the Monte Perdido Glacier is likely to provide
2 important information on the year-to-year response of its mass balance to to a wide
3 variety of climatic conditions, and will allow detailed analysis of the role of positive and
4 negative feedbacks in this much deteriorated glacier. Thus, study of this glacier may
5 serve as a model for studies of the evolution of glaciers in other regions of the world
6 that have similar characteristics now and in the future.

7 8 **Acknowledgements**

9 This study was funded by two research grants: “CGL2014-52599-P, *Estudio del manto*
10 *de nieve en la montaña española, y su respuesta a la variabilidad y cambio climatico*”
11 (IBERNIEVE-Ministry of Economy and Competitivy), and “*El glaciar de Monte*
12 *Perdido: estudio de su dinámica actual y procesos criosféricos asociados como*
13 *indicadores de procesos de cambio global*” (MAGRAMA 844/2013). The authors are
14 grateful for the support provided by the “Dirección General de Conservación del Medio
15 Natural (Government of Aragón)” and to the staff of the Ordesa and Monte Perdido
16 National Park during our field campaigns.

References

- Abermann, J., Lambrecht, A., Fischer, A., and Kuhn, M.: Quantifying changes and trends in glacier area and volume in the Austrian Ötztal Alps (1969–1997–2006). *The Cryosphere*, 3, 205–215, 2009.
- Arenillas, M., Cobos, G., Navarro, J.: Datos sobre la nieve y los glaciares en las cordilleras españolas. El programa ERHIN (1984-2008). Ed. Ministerio de Medio Ambiente y Medio Rural y Marino, Madrid, 231pp, 2008.
- Beniston M.: Climatic change in mountain regions: a review of possible impacts. *Climatic Change*, 59, 5–31, 2003.
- Boyé, M.: Névés et érosion glaciaire.: *Revue de Géomorphologie Dynamique* 2, 20–36, 1952.
- Buisan, S.T., Saz, M.A., López-Moreno, J.I.: Spatial and temporal variability of winter snow and precipitation days in the western and central Spanish Pyrenees. *International Journal of Climatology*, 35 (2), 259–274, 2015.
- Buisan, S.T., López-Moreno, J.I., Saz, M.A., Kochendorfer, J.: Impact of weather type variability on winter precipitation, temperature and snowpack in the Spanish Pyrenees. *Climate Reserach*, under review.
- Büngten, U., Frank, D., Grudd, H., Esper, J.: Long-term summer temperature variations in the Pyrenees. *Clymate Dynamics*, 31 (6), 615–631, 2008.
- Carrivick, J. L. and Brewer, T. R.: Improving local estimations and regional trends of glacier equilibrium line altitudes. *Geografiska Annaler: Series A, Physical Geography*, 86: 67–79, 2004.

1 Carturan, L., Filippi, R., Seppi, R., Gabrielli, P., Notarnicola, C., Bertoldi, L.,
 2 Paul, F., Rastner, P., Cazorzi, F., Dinale, R., and Dalla Fontana, G.: Area and volume
 3 loss of the glaciers in the Ortles-Cevedale group (Eastern Italian Alps): controls and
 4 imbalance of the remaining glaciers, *The Cryosphere*, 7, 1339-1359, 2013a.

5 Carturan, L., Baroni, C., Becker, M., Bellin, A., Cainelli, O., Carton, A., Casarotto,
 6 C., Dalla Fontana, D., Godio, A., Martinelli, T., Salvatore, M.C., Seppi, R.: Decay of
 7 a long-term monitored glacier: Careser Glacier (Ortles-Cevedale, European Alps).
 8 *The Cryosphere*, 7, 1819-1838, 2013b.

9 Carturan L., Baldassi, G.A., Bondesan, A., Calligaro, S., Carton, A., Cazorzi F.,
 10 Dalla Fontana, G., Francese, R., Guarnieri, A., Milan, N., Moro, D. Tarolli, P.:
 11 Current behavior and dynamics of the lowermost Italian glacier (Montasio
 12 Occidentale, Julian Alps). *Geografiska Annaler: Series A, Physical Geography*,
 13 95(1), 79-96, 2013c.

14 Chueca, J., Julián, A.: Relationship between solar radiation and the development and
 15 morphology of small cirque glaciers (Maladeta Mountain massif, Central Pyrenees,
 16 Spain). *Geografiska. Annaler*, 86 A (1), 81-89, 2004.

17 Chueca, J., Julián, A., Saz, M.A., Creus, J., López-Moreno, J.I.: Responses to
 18 climatic changes since the Little Ice Age on Maladeta Glacier (Central Pyrenees).
 19 *Geomorphology*, 68(3–4), 167–182, 2005.

20 Chueca, J., Julián A., López-Moreno, J.I.: Recent evolution (1981–2005) of the
 21 Maladeta glaciers, Pyrenees, Spain: extent and volume losses and their relation with
 22 climatic and topographic factors. *Journal of Glaciology*, 53 (183), 547-557, 2007.

Chueca, J., Julián Andrés, A., López Moreno, J.I.: The retreat of the Pyrenean
 Glaciers (Spain) from the Little Ice Age: data consistency and spatial differences.
 Terra Glacialis, 2008, 137-148, 2008.

Cogley, J.G.: Geodetic and direct mass-balance measurements: comparison and joint
 analysis. *Annals of Glaciology*, 50(50), 96-100, 2009.

Deaux, N., Soubayroux, J. M., Cuadrat, J. M., Cunillera, J., Esteban, P., Prohom, M.,
 and Serrano-Notivoli, R.: Homogénéisation transfrontalière des températures sur le
 massif des Pyrénées, XXVII Colloque de l'Association Internationale de
 Climatologie, 2–5 Julliet 2014, Dijon, France, 344–350, 2014.

Del Río, M., Rico, I., Serrano, E., Tejado, J.J.: Applying GPR and Laser Scanner
 Techniques to Monitor the Ossoue Glacier (Pyrenees). *Journal of Environmental &
 Engineering Geophysics*, 19 (4), 239–248, 2014.

Dessens, J. and Bücher, A.: Changes in minimum and maximum temperatures at the
 Pic du Midi in relation with humidity and cloudiness, 1882–1984. *Atmospheric
 Research*, 37, 147–162, 1995.

Egli, L., Griessinger, N., Jonas, T.: Seasonal development of spatial snow depth
 variability across different scales in the Alps. *Annals of Glaciology*, 52 (58), 216-
 222, 2011.

Favey, E., Wehr, A., Geiger, A., Kahle. H.G.: Some examples of European activities
 in airborne laser techniques and an application in glaciology. *Journal of
 Geodynamics*, 34, 347-355, 2002.

1 Fay, M.P.: Proschan, M.A.: Wilcoxon–Mann–Whitney or t-test? On assumptions for
2 hypothesis tests and multiple interpretations of decision rules. *Statistics Surveys* 4:
3 1–39, 2010.

4 Feuillet, Th. and Mercier, D.: Post-Little Ice Age patterned ground development on
5 two Pyrenean proglacial areas: from deglaciation to periglaciation. *Geografiska*
6 *Annaler: Series A*, 94, 363–376, 2012.

7 Fischer, M., Huss, M., Hoelzle, M.: Surface elevation and mass changes of all Swiss
8 glaciers 1980–2010. *The Cryosphere*, 9, 525–540, 2015.

9 García Ruiz, J.M., Martí Bono, C.E.: Mapa geomorfológico del Parque Nacional de
10 Ordesa y Monte Perdido. Organismo Autónomo de Parques Nacionales, Madrid, 106
11 pp, 2002.

12 García-Ruiz, J.M., Palacios D., De Andrés N, Valero-Garcés BL, López-Moreno JI,
13 Sanjuán Y.: Holocene and ‘Little Ice Age’ glacial activity in the Marboré Cirque,
14 Monte Perdido Massif, Central Spanish Pyrenees. *The Holocene* 24 (11), 1439–1452,
15 2014.

16 Gardent, M., Rabatel, A., Dedieu, J.P., and Deline, P.: Multi-temporal glacier
17 inventory of the French Alps from the late 1960s to the late 2000s, *Global and*
18 *Planetary Change*, 120, 24–37, 2014.

19 Gellatly A.F., Grove, J.M., Bücher, A., Latham, R., Whalley, W.B.: Recent historical
20 fluctuations of the Glacier du Taillon. *Physical Geography*, 15 (5), 399–413, 1995.

21 Gómez de Llarena, J.: Algunos datos sobre el glaciar actual del Monte Perdido
22 (Pirineos). *Boletín de la Real Sociedad Española de Historia Natural* 36, 327–343,
23 1936.

Gómez-Ortiz, A., Oliva, M., Salvador-Franch, F., Salvà-Catarineu, M., Palacios, D., de Sanjosé-Blasco, J.J., Tanarro-García, L.M., Galindo-Zaldívar, J., Sanz de Galdeano, C.: Degradation of buried ice and permafrost in the Veleta cirque (Sierra Nevada, Spain) from 2006 to 2013 as a response to recent climate trends. *Solid Earth* 5, 979-993, 2014.

González Trueba, J.J., Martín Moreno, R., Martínez de Pisón, E., Serrano E.: Little Ice Age glaciation and current glaciers in the Iberian Peninsula. *The Holocene* 18 (4), 569–586, 2008.

Grunewald, K., Scheithauer, J.: Europe's southernmost glaciers: response and adaptation to climate change. *Journal of Glaciology*, 56 (195), 129-142, 2010.

Grünwald, T., Schirmer, M., Mott, R., and Lehning, M.: Spatial and temporal variability of snow depth and ablation rates in a small mountain catchment, *The Cryosphere*, 4, 215-225, 2010.

Haeberli, W.: Glacier fluctuations and climate change detection. *Geografia Fisica e Dinamica Quaternaria*, 18, 191-195, 1995.

Haeberli, W., Beniston, M.: Climate change and its impacts on glaciers and permafrost in the Alps. *Ambio*, 27 (4), 258-265, 1998.

Hernández-Pacheco, F., Vidal Box, C.: La tectónica y la morfología del macizo de Monte Perdido y de las zonas de cumbres inmediatas en el pirineo Central. *Pirineos* 4, 69-108, 1946.

Huss, M., Hock, R., Bauder A., Funk M.: 100-year mass changes in the Swiss Alps linked to the Atlantic Multidecadal Oscillation. *Geophys. Res. Lett.*, 37, L10501, 2010.

- Julián, A., Chueca J.: Pérdidas de extensión y volumen en los glaciares del macizo de Monte Perdido (Pirineo central español): 1981-1999. *Boletín Glaciológico Aragonés*, 8, 31-60, 2007.
- Kenawy, A., López-Moreno, J.I., Vicente-Serrano, S.M.: Trend and variability of surface air temperature in northeastern Spain (1920–2006): linkage to atmospheric circulation. *Atmospheric Research*. 106, 159-180, 2012.
- Kendall, M.G., J. D. Gibbons. Rank correlation methods. Oxford University Press, 272 pp, 1990.
- López Moreno, J.I.: Los glaciares del alto valle del Gállego (Pirineo central) desde la Pequeña Edad de Hielo. Implicaciones en la evolución de la temperatura, Geoforma Ediciones, Logroño, 77 p, 2000.
- López-Moreno, J.I. Recent variations of snowpack depth in the central Spanish Pyrenees. *Arctic Antarctic and Alpine Research*, 37 (2), 253–260, 2005.
- López-Moreno, J. I., Nogués-Bravo D, Chueca-Cía J., Julián-Andrés A.: Change of topographic control on the extent of cirque glaciers since the Little Ice Age. *Geophysical Research Letters*, 33, L24505, 2006.
- López-Moreno, J. I., García-Ruiz, J. M., and Beniston, M.: Environmental Change and water management in the Pyrenees. Facts and future perspectives for Mediterranean mountains. *Global and Planetary Change*, 66(3–4), 300–312, 2008.
- López-Moreno, J.I., Fontaneda, S., Bazo, J., Revuelto, J., Azorín-Molina, C., Valero-Garcés, B., Morán-Tejeda, E., Vicente-Serrano, S.M., Zubieta, R., Alejo-Cochachín, J.: Recent glacier retreat and climate trends in cordillera Huaytapallana, Peru. *Global and Planetary Change*, 112,1-12, 2014.

Macias, D., Stips, A., Garcia-Gorriz, E.: Application of the Singular Spectrum Analysis Technique to Study the Recent Hiatus on the Global Surface Temperature Record. PLoS ONE, 9 (9), 2014.

Marshall S.: Glacier retreat crosses a line. Science, 345 (6199), 872, 2014

Martín Moreno, R.: Comparación de dos glaciares: Longyearbeen (Spitsbergen) y Monte Perdido (Pirineos). Características y evolución desde la Pequeña Edad del Hielo. Ería 63, 5-22, 2004.

Marti, R., Gascoin, S., Houet, T., Ribière, O., Laffly, D., Condom, T., Monnier, S., Schmutz, M., Camerlynck, C., Tihay, J.P., Soubeyroux, S.M., René, P.: Evolution of Ossoue Glacier (French Pyrenees) since the end of the Little Ice Age. The Cryosphere Discussions, 9, 2431-2494, 2015.

Martínez de Pisón, E., Arenillas, M.: Los glaciares actuales del pirineo español. En La nieve en el pirineo español. MOPU, Madrid, 287 pp. 29-98, 1988.

Marzeion, B., Cogley, J. G., Richter, K., and Parkes, D.: Attribution of global glacier mass loss to anthropogenic and natural causes, Science, 345, 919–921, 2014.

Marzeion, B., Leclercq, P.W., Cogley, J.G., Jarosch, A.H.: Global glacier mass loss reconstructions during the 20th century are consistent. The Cryosphere, 9, 2399-2404, 2015.

Mernild, S.H., Lipscomb, W.H., Bahr, D.B., Radic, V., Zemp, M.: Global glacier changes: a revised assessment of committed mass losses and sampling uncertainties. The Cryosphere 7:1565-1577, 2013.

1 Nicolás, P.: Morfología del circo de Tucarroya. Macizo de Monte Perdido, Pirineo
2 Aragón. Cuadernos de Investigación Geográfica, 7, 51-80, 1981.

3 Nicolás, P.: Morfología de un aparato glaciar: el glaciar nororiental de Monte Pedido.
4 Pirineo de Huesca. In: Atlas de Geomorfología. Alianza Editorial, Madrid, pp. 189-
5 207, 1986.

6 Nogués-Bravo, D., Lasanta, T., López-Moreno, J.I., Araujo: Climate change in
7 Mediterranean mountains during the 21st century. *Ambio*, 37(4), 280–285, 2008.

8 Oliva-Urcía, B., Moreno, A., Valero-Garcés, B., Mata, P.: Magnetismo y cambios
9 ambientales en registros terrestres: el lago de Marboré, Parque Nacional de Ordesa y
10 Monte Perdido (Huesca). *Cuadernos de Investigación Geográfica* 39 (1), 117-140,
11 2013.

12 Pelto, M.S. : Forecasting temperate alpine glacier survival from accumulation zone
13 observations. *The Cryosphere* 3: 323-350, 2010.

14 Prokop, A.: Assessing the applicability of terrestrial laser scanning for spatial snow
15 depth measurements. *Cold Regions Science and Technology*, 54 (3), 155–163, 2008.

16 Qu, B., Ming, J., Kang, S.-C., Zhang, G.-S., Li, Y.-W., Li, C.-D., Zhao, S.-Y., Ji, Z.-
17 M., and Cao, J.-J.: The decreasing albedo of the Zhadang glacier on western
18 Nyainqentanglha and the role of light-absorbing impurities, *Atmos. Chem. Phys.*, 14,
19 11117-11128, doi:10.5194/acp-14-11117-2014, 2014.

20 Reinwarth, O., Escher-Vetter, H.: Mass Balance of Vernagtferner, Austria, From
21 1964/65 to 1996/97: Results for Three Sections and the Entire Glacier. *Geografiska*
22 *Annaler: Series A, Physical Geography*, 81: 743–751, 1999. René, P.: *Le*
23 *réchauffement climatique en images*. Ed. Cairn. Pau (France), 167 pp, 2013.

Reshetyuk, Y.: Calibration of Terrestrial Laser Scanners Callidus 1.1, Leica HDS 3000 and Leica HDS 2500. *Survey Review*, 38 (302), 703-713, 2006.

Revuelto, J., López-Moreno J.I., Azorín-Molina C., Zabalza J., Arguedas G., Vicente-Serrano S.M.: Mapping the annual evolution of snow depth in a small catchment in the Pyrenees using the long-range terrestrial laser scanning. *Journal of Maps*, 10 (3), 359-373, 2014.

Rolstad, C., Haug, T. and Denby, B.: Spatially integrated geodetic glacier mass balance and its uncertainty based on geostatistical analysis: application to the western Svartisen ice cap, Norway. *Journal of Glaciology*, 55 (192), 666-680, 2009.

Sanjosé, J.J.; Berenguer, F.; Atkinson, A.D.J.; De Matías, J.; Serrano, E.; Gómez-Ortiz, A.; González-García, M.; Rico, I.: Geomatics techniques applied to glaciers, rock glaciers and ice-patches in Spain (1991-2012). *Geografiska Annaler, Series A, Physical Geography* 96, 3, 307-321, 2014.

Schwalbe, E., Maas, H.-G., Dietrich, R., Ewert, H.: Glacier velocity determination from multi-temporal long range laser scanner point clouds. *International Archives of Photogrammetry and Remote Sensing*, 18, B5, 2008.

Scotti, R., Brardinoni, F., Crosta, G.B.: Post-LIA glacier changes along a latitudinal transect in the Central Italian Alps. *The Cryosphere* 8, 2235-2252, 2014.

Schrader, F. Carte du Mont-Perdu et de la region calcaire des Pyrénées. *Expart des Mémoires de la Société des Sciences Physiques et Naturelles de Bordeaux*. Bordeaux, Journal de L'imprimerie Chariol, 1874.

Serrano, E., González-Trueba, J.J., Sanjosé, J.J., Del Río, L.M. Ice patch origin, evolution and dynamics in a temperate high mountain environment: the Jou Negro, Picos de Europa (NW Spain). *Geografiska Annaler-A*, 93 (2), 57-70, 2011.

1 Vicente-Serrano, S. M., Trigo, R. T., López-Moreno, J. I., Liberato, M. L. R.,
2 Lorenzo-Lacruz, J., Beguería, S.: The 2010 extreme winter north hemisphere
3 atmospheric variability in Iberian precipitation: anomalies, driving mechanisms and
4 future projections. *Climate Research*, 46, 51–65, 2011

5 Vincent, C., Ramanathan, A.L., Wagnon, P., Dobhal, D.P., Linda, A., Berthier, A.,
6 Sharma, P., Arnaud, Y. F., Azam, M., Gardelle J.: Balanced conditions or slight mass
7 gain of glaciers in the Lahaul and Spiti region (northern India, Himalaya) during the
8 nineties preceded recent mass loss. *The Cryosphere* 7: 569-582, 2013.

9 Zemp et.al. Historically unprecedented global glacier decline in the early 21st
10 century. *Journal of Glaciology*, 61 (228), 745-762, 2015.

Figure captions

Figure 1. Monte Perdido study area and extent of ice cover at the end of the Little Ice Age (according to the map of Schrader [1874]) and in 2008. Red square marks the scanning positions, numbered points indicate the position of the fixed targets used for georeferencing and merging the different clouds of points.

Figure 2. Interannual fluctuations and overall trends (straight lines) of minimum and maximum air temperatures during the accumulation and ablation periods, precipitation during the accumulation period, and maximum snow depth during April based on data from the Goriz meteorological station (1983 to 2014). Boxplots at the right of each panel show the interannual variability during the most recent 3 years (2011/12, 2012/13, and 2013/14) when terrestrial laser scanning measurements were available. Box: 25th and 75th percentiles, bars: 10th and 90th percentiles, dots: 5th and 95th percentiles, black line: median, red line: average.

Figure 3. Interannual fluctuations of minimum and maximum air temperatures during the accumulation and ablation periods and precipitation during the accumulation period at the stations of Aragnouet, Canfranc, Mediano (only temperature) and Pineta (only precipitation) during the period 1955-2013. Numbers give the Tau-b values of the trends. Asterisks indicate statistically significant trends (<0.05)

Figure 4. Photographs of the Monte Perdido Glacier during the late summer of 1981 and 2011.

Figure 5. Changes in glacier elevation in the upper and lower Monte Perdido Glacier from 1981 to 1999 and from 1999 to 2010 based on comparison of DEMs.

Figure 6. Changes in glacier elevation based on terrestrial laser scanning from September of 2011 to 2012 (Fig. 5A), 2012 to 2013 (Fig 5B), 2013 to 2014 (Fig. 5C), and 2011 to 2014 (Fig. 5D).

Figure 7. Changes in glacier elevation over the whole glacier, lower glacier, and upper glacier for the same 4 time periods examined in Figure 5. Box: 25th and 75th percentiles, black line: median, red line: average, bars: 10th and 90th percentiles, dots: 5th and 95th percentiles.

1 **Table 1.** Tau-b values of the trends for the period 1983-2013 for temperature and precipitation in the analyzed stations. Asterisks indicate
2 statistically significant trends ($p < 0.05$). Bold numbers are statistically significant differences in the medians of the period 1982-1999 and 1999-
3 2010 according to the Mann-Whitney test.

	Aragnouet			Canfranc			Mediano		Pineta	Góriz		
	Tmx	Tmn	Precip	Tmx	Tmn	Precip	Tmx	Tmn	Precip	Tmx	Tmn	Precip
January	0.08	0.02	0.04	-0.03	-0.13	0.03	0.06	0.04	0.06	0.07	0.11	0.02
February	0.04	0.06	0.02	0.05	-0.01	-0.08	0.03	-0.03	0.39*	0.04	0.02	0.00
March	0.11	0.11	0.14	0.03	-0.03	0.26	-0.02	0.03	0.31	0.02	0.06	0.20
April	0.28*	0.25	0.08	0.24	0.19	-0.15	0.02	0.12	0.02	0.15	0.21	-0.17
May	0.23	0.24	0.31*	0.30*	0.18	0.14	-0.01	0.04	0.12	0.34*	0.33*	0.27
June	0.28*	0.31*	0.14	0.35*	0.47*	0.04	0.09	-0.05	0.10	0.32*	0.25*	-0.05
July	-0.12	0.06	0.13	0.11	0.15	0.16	-0.07	-0.21	0.15	-0.07	-0.05	-0.11
August	0.07	0.13	-0.02	-0.02	0.01	0.03	-0.12	-0.25	0.32	0.10	0.07	-0.02
September	0.05	0.05	0.02	-0.06	-0.23	0.10	-0.18	-0.23	0.10	0.01	-0.02	0.04
October	0.08	0.19	0.19	0.06	0.04	0.14	0.04	-0.14	0.08	0.01	0.04	0.11
November	-0.06	-0.06	0.18	-0.18	-0.23	0.10	-0.08	-0.30*	-0.02	-0.11	-0.09	0.00
December	-0.15	-0.10	-0.03	-0.37*	-0.42*	0.08	-0.25	-0.23	0.13	-0.27*	-0.23	-0.06
Accumulation period	0.10	0.11	0.12	0.04	0.11	0.01	-0.22	-0.22	0.00	0.06	0.15	0.05
Ablation period	0.10	0.10		0.17	0.11		-0.26	-0.26		0.13	0.12	

4

5 **Table 2.** Surface area (ha), loss of surface area (ha), and annual rate of surface area loss (ha yr^{-1}) of the Monte Perdido Glacier.

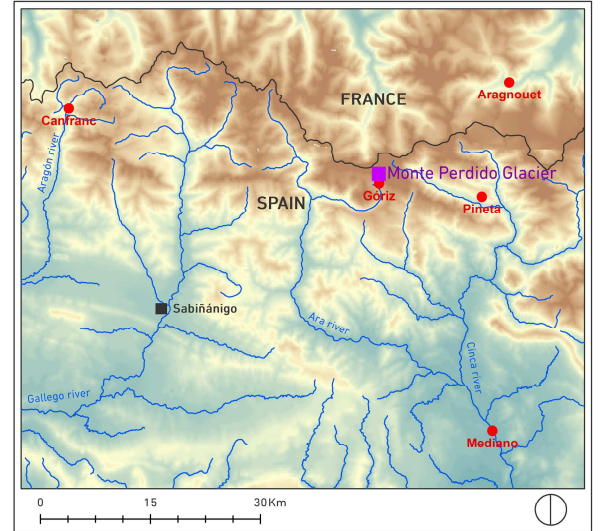
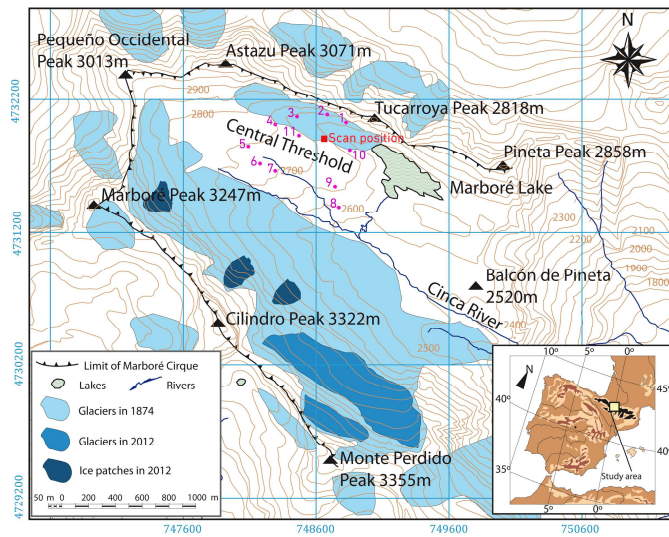
6

	Surface Area			Loss of Surface Area	
	1981	1999	2006	1981-1999	1999-2006

Upper glacier (ha)	8.30±0.27	6.80±0.25	4.80±0.21	1.50±0.47	2.00±0.46
Lower glacier (ha)	40.10±0.59	37.10±0.62	33.70±0.54	3.0±1.21	3.40±1.16
Entire glacier (ha)	48.40±0.65	43.90±0.62	38.50±0.58	4.50±1.23	5.40±1.20
Entire glacier (ha yr ⁻¹)				0.25±0.07	0.77±0.17

1

2

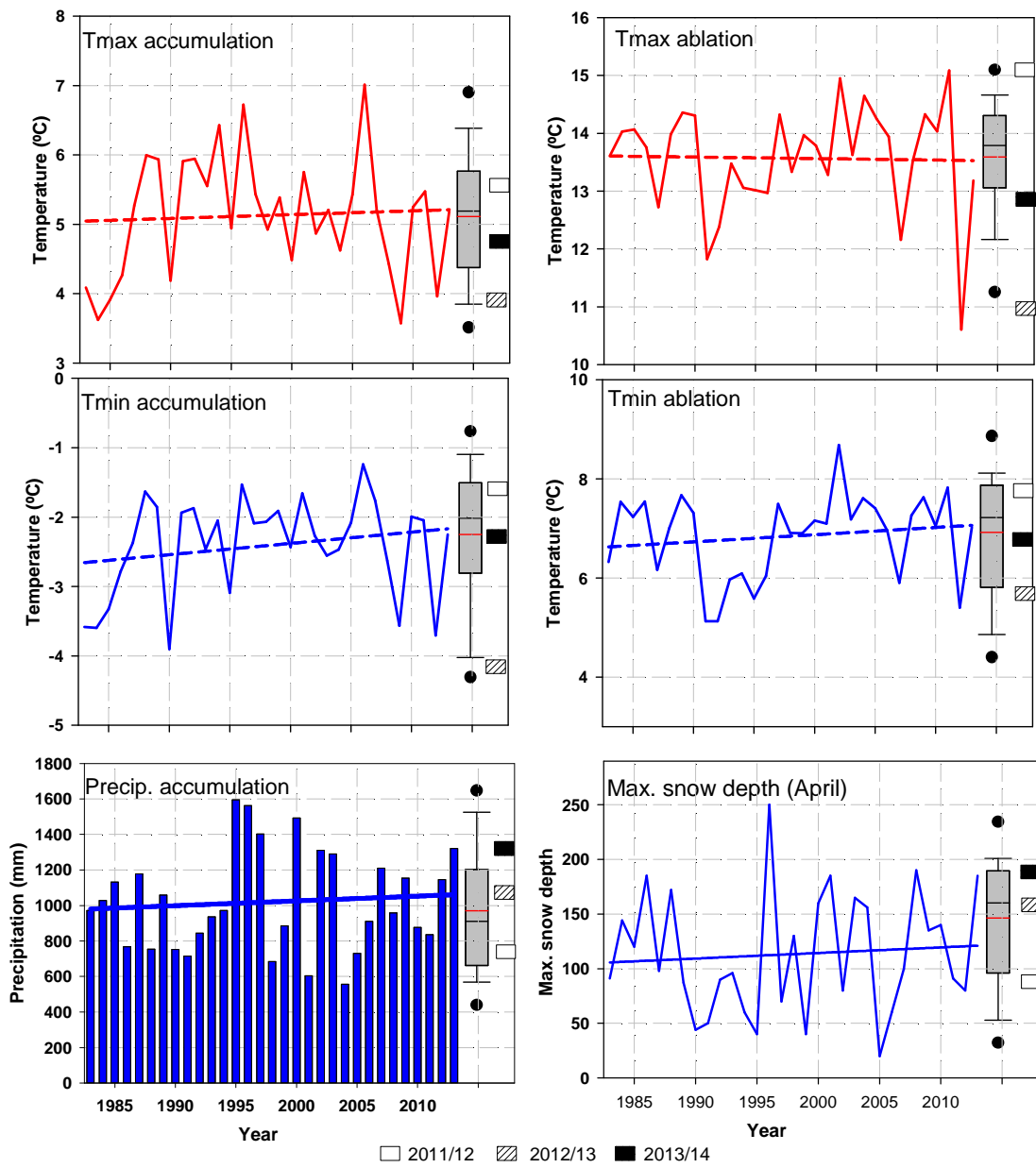


1

2 Figure 1.

3

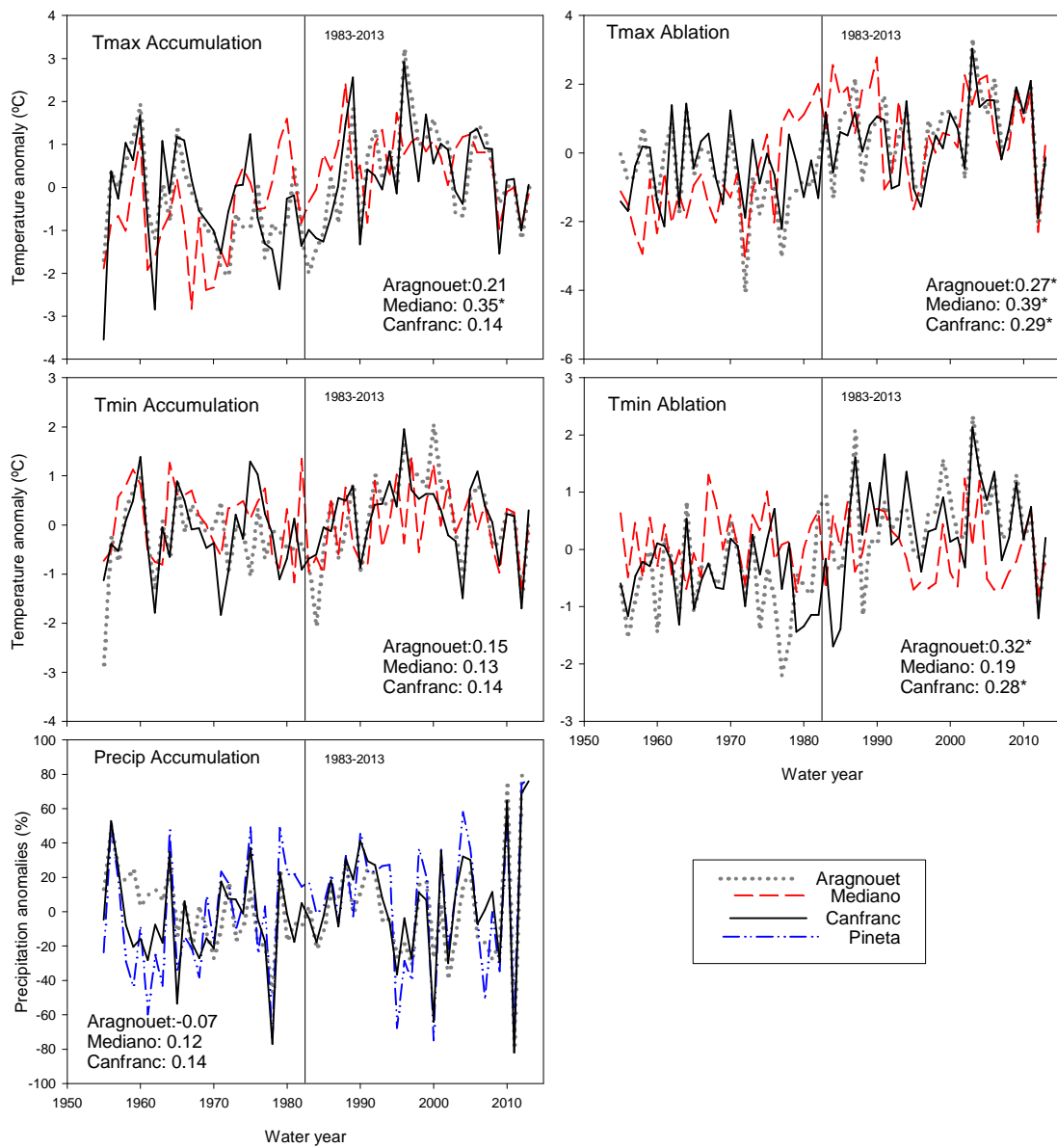
1



2

3 **Figure 2.**

4



1

2 **Figure 3.**

3

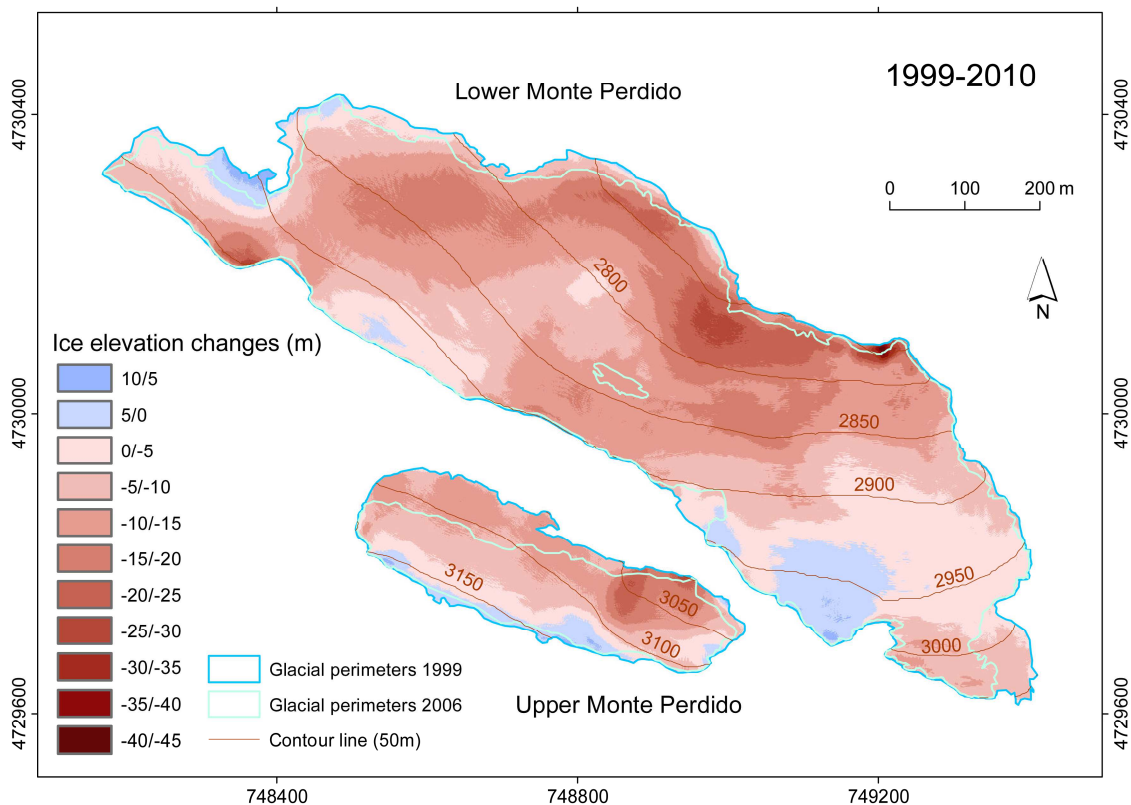
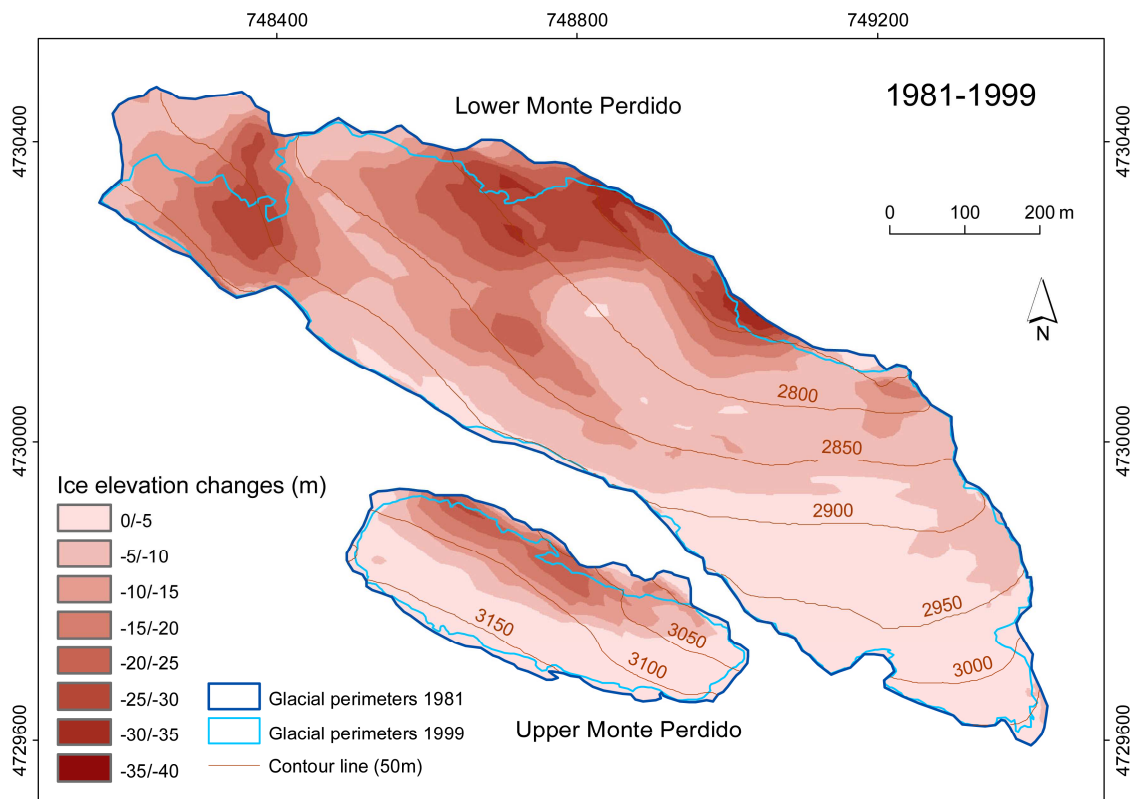


1

2 **Figure 4.**

3

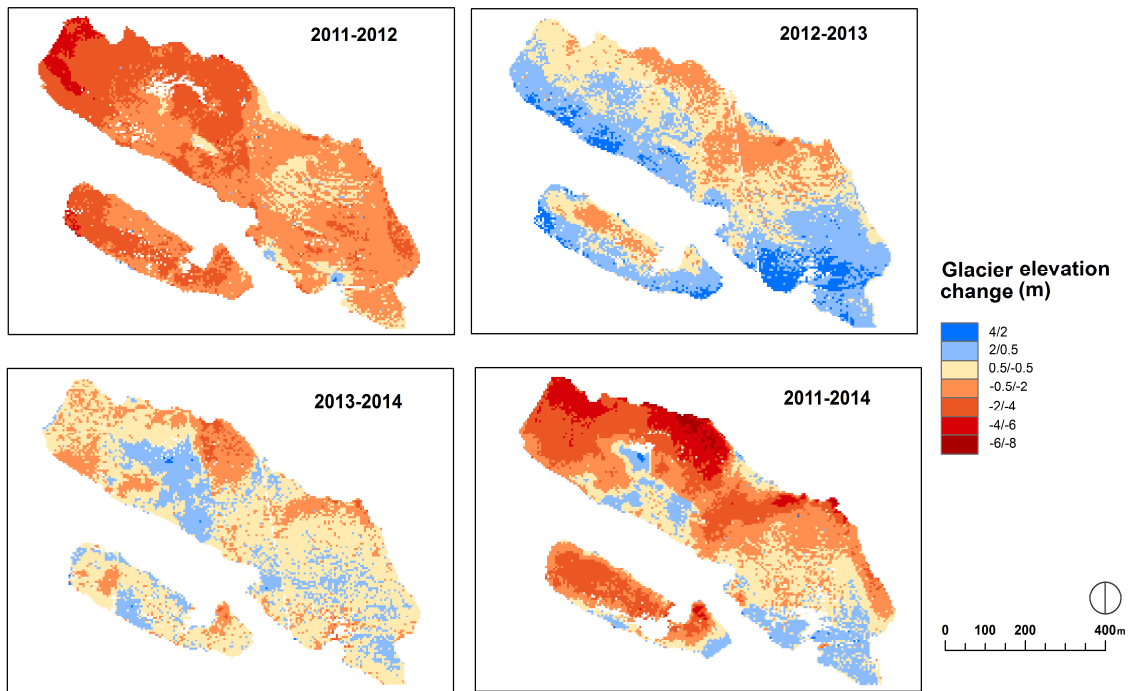
4



1

2 **Figure 5.**

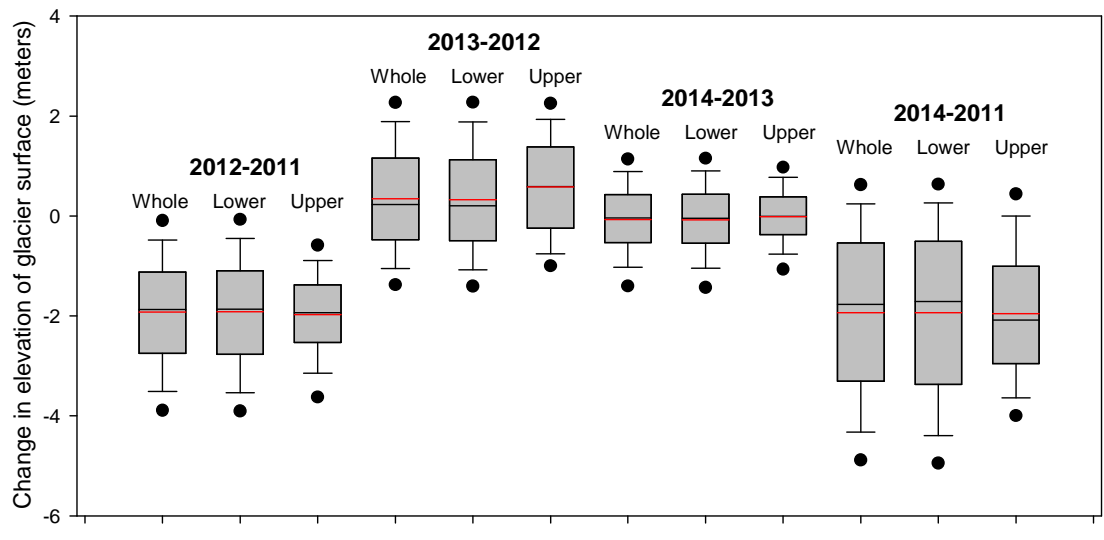
3



1

2 **Figure 6.**

1



2

3 **Figure 7.**

4

5

6

7